

**OPEN ACCESS**

## (e, 2e) Study of Ca in Coplanar Symmetric Geometry at low impact energies using Distorted Wave Born Approximation

To cite this article: S Sunil Kumar *et al* 2007 *J. Phys.: Conf. Ser.* **80** 012021

View the [article online](#) for updates and enhancements.

### Related content

- [The TDCS of ionic targets in the coplanar to perpendicular plane geometry](#)  
Y Khajuria, L Q Chen, X J Chen *et al.*
- [Post-collision interactions and the polarization effect in \(e, 2e\) collisions of helium](#)  
Zang Shuang-Shuang and Ge Zi-Ming
- [Post collision interaction effects in the ionisation of helium by electron impact](#)  
H Ray and A C Roy

### Recent citations

- [The Distorted-Wave Born Approach for Calculating Electron-Impact Ionization of Molecules](#)  
Don H. Madison and Ola Al-Hagan



**IOP | ebooks™**

Bringing together innovative digital publishing with leading authors from the global scientific community.

Start exploring the collection—download the first chapter of every title for free.

## (e, 2e) Study of Ca in Coplanar Symmetric Geometry at low impact energies using Distorted Wave Born Approximation

S Sunil Kumar<sup>1</sup>, Y Khajuria<sup>2</sup>, and P C Deshmukh<sup>1</sup>

<sup>1</sup> Department of Physics, Indian Institute of Technology, IIT Madras, Chennai-36, India

<sup>2</sup> School of Applied Physics and Mathematics, SMVDU, Kakryal, J&K, India

E-mail: sunilks@physics.iitm.ac.in

**Abstract.** The triple differential cross section of Ca ( $4s^2$ ) in coplanar symmetric geometry at low impact energies is calculated using a spin averaged static exchange potential and a modified semi-classical exchange potential in Distorted Wave Born Approximation. The calculations have been carried out at incident energies of 10.11, 12.61, 19.61, 24.61, 34.61, 44.61, 54.61 and 64.61 eV for Ca, at which experimental data were available for comparison. The effect of post collision interaction has also been studied using Gamow factor introduced by Whelan et al. (1994). The present calculations have been compared with the recent (e, 2e) experimental studies of Murray (2005) and the earlier theoretical work of Chauhan et al. (2005). The present results are found to be in better agreement with experimental data as compared to the earlier study.

### 1. Introduction

The electron-impact ionization of atoms is one of the most fundamental and exciting processes in atomic physics. Wide range of kinematic situations that are available to the three body final state in such a process provides an extremely interesting diversity of phenomena. Great deal of information can be obtained from the (e, 2e) processes by coincidence detection of the two outgoing electrons. As the triple differential cross section in such a process is a function of several variables such as energy of the incident electron, and energies and directions of emission of outgoing electrons, the process is studied under various simple special kinematical arrangements. The most general kinematic situation for an (e, 2e) reaction is shown in Figure 1. In the coplanar asymmetric geometry the momenta  $\mathbf{k}_0$ ,  $\mathbf{k}_1$ , and  $\mathbf{k}_2$  of the incident, scattered and ejected electrons respectively are in the same plane ( $\phi = 0$ );  $\theta_1$  (scattering angle) is kept normally small (generally less than about  $30^\circ$ ), and  $\theta_2$  (ejected electron angle) is varied. In the non-coplanar geometry  $\mathbf{k}_2$  is out of the reference plane ( $\mathbf{k}_0, \mathbf{k}_1$ );  $\theta_1 = \theta_2 = \theta$  is fixed (usually at  $45^\circ$ ) and  $\phi$  is varied. In the coplanar symmetric geometry, again momenta  $\mathbf{k}_0$ ,  $\mathbf{k}_1$ , and  $\mathbf{k}_2$  are in the same plane ( $\phi = 0$ ) and (scattering angle)  $\theta_1 = \theta_2 = \theta$  is varied. Another important distinction is made between asymmetric and symmetric geometries; in the asymmetric case, a fast electron is detected in coincidence with the slow electron, while

in the symmetric geometry the energies of the two outgoing electrons are kept the same ( $E_1 = E_2$ ). We have employed the coplanar symmetric geometry in which the incident and outgoing electrons are in the same plane; both the ejected and scattered electrons make equal angles with the incident direction and have equal energies.

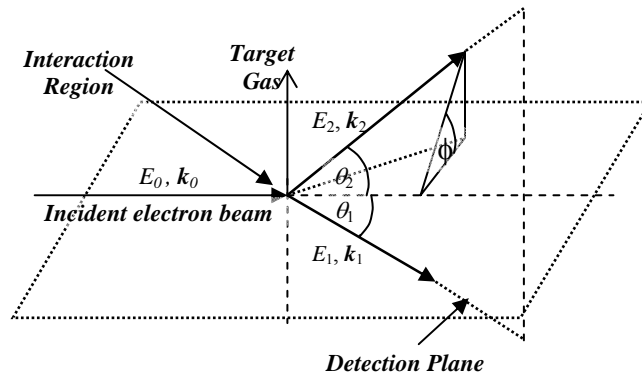


**Figure 1.** The complete kinematical arrangement for an (e, 2e) scattering.

The (e, 2e) technique has been applied to a wide range of targets and kinematical arrangements since the first experimental studies of this type by Ehrhardt et al. [1] and Amaldi et al. [2]. Their results provided a qualitative understanding of the process in developing suitable models. Since then attention has largely been confined to the coplanar collisions. Such experiments, in which the kinematics of the collision are completely determined, provide the most complete test of theories of (e, 2e) reactions to study in detail the collision dynamics of single ionization process and a possible powerful analytical tool to probe the electronic structure. The testing and the development of the current theoretical models have been further challenged by including the wide range of kinematical options employed for instance by Pochat et al. [3], Hawley-Jones et al. [4], Röder et al. [5], Murray [6] and Murray and Read [7-11]. The recent experiments in the coplanar geometry on alkaline earth metal and alkali earth metal targets of Murray and Cvejanovic [12] and Murray [13] have evoked a fresh interest in this problem.

The Distorted Wave Born Approximation (DWBA) is well known and has been shown to be capable of predicting accurate (e, 2e) cross sections for a wide variety of atomic targets above around 50 eV (Whelan et al. [14], Khajuria and Tripathi [15]). Major features which have made the DWBA so successful are the inclusion of final state electron–electron interaction, known as Post Collision Interaction (PCI), which results due to the electrostatic Coulomb repulsion between the outgoing electrons. Electron exchange interaction and polarization effects are known to be very important at low energies. Allen et al. [16] noticed that the inclusion of the Post Collision Interaction (PCI) and polarization of atomic targets play important role in determining atomic structure. Rioual et al. [17] have found that the inclusion of polarization effect and PCI leads to the better agreement for neon and argon. Excellent agreement between experiment and theory with PCI and polarization potential at the energies  $\sim 1.8$  to 2.2 times the ionization threshold of hydrogen in coplanar symmetric geometry has been observed by Whelan et al. [18].

Recently, Chauhan et al. [19] have carried out studies on the electron impact ionization of Ca ( $4s^2$ ) at low impact energies using DWBA in coplanar symmetric geometry. They have studied the effects of exchange distortion through the spin averaged static exchange potential of Furness and McCarthy [20] and post collision interaction, through angle dependent

effective charges. Although their results qualitatively reproduced many of the features of the cross section and showed agreement with the experimental results, significant discrepancies are noticed, such as the inability of their method to reproduce the three peak structure at the lowest impact energy when PCI is not included.

In the present paper, DWBA with spin averaged local static exchange potential of Furness and McCarthy [20] and a modified semiclassical exchange potential (MSCEP) of Gianturco and Scialla [21] has been employed to study the triple differential cross section of calcium in the coplanar symmetric geometry. The effect of post collision interaction has been studied through Gamow factor [18, 22], which is a simple symmetric function of angle between the outgoing electrons in coplanar symmetric geometry (Figure 2). It is observed that both the potentials reproduce most of the features of the triple differential cross section in agreement with the experimental results except for higher angle ranges at certain impact energies.

## 2. Theory

The triple differential cross section is a measure of the probability that an (e,2e) reaction (Figure 1) at an incident electron of energy  $E_0$  and momentum  $\mathbf{k}_0$ , upon collision with the target produces two electrons (emitted and scattered) with energies  $E_1$  and  $E_2$  having respective momenta  $\mathbf{k}_1$  and  $\mathbf{k}_2$  satisfying the energy relation

$$E_0 = E_1 + E_2 + I, \quad (1)$$

where  $I$  is the ionization potential of the target atom.

The triple differential cross section for the coincidence detection of the two continuum electrons emerging into the directions defined by solid angles  $\Omega_1$  and  $\Omega_2$  takes the form (in atomic units)

$$\frac{d^3\sigma}{d\Omega_1 d\Omega_2 dE_1} = (2\pi)^4 \frac{k_1 k_2}{k_0} \sum_{av} (|f|^2 + |g|^2 - \text{Re}(f^* g)). \quad (2)$$

Here,  $\sum_{av}$  represents the sum over the final and average over the initial magnetic and spin degeneracies. Also,  $f$  and  $g$  are respectively direct and exchange amplitudes for the ionization processes and are given by

$$f \equiv \langle \chi^{(-)}(\mathbf{k}_1, \mathbf{r}_1) \chi^{(-)}(\mathbf{k}_2, \mathbf{r}_2) | V_{12} | \chi^{(+)}(\mathbf{k}_0, \mathbf{r}_1) \psi_{nl} \rangle, \quad (3)$$

and

$$g \equiv \langle \chi^{(-)}(\mathbf{k}_1, \mathbf{r}_2) \chi^{(-)}(\mathbf{k}_2, \mathbf{r}_1) | V_{12} | \chi^{(+)}(\mathbf{k}_0, \mathbf{r}_1) \psi_{nl} \rangle.$$

In the above equations,  $V_{12}$  represents the interaction potential between the incident and target electrons responsible for the ionization.  $\psi_{nl}$  represents the valence  $nl$  orbital of the target. The orbitals  $\psi_{nl}$  have been taken from the Hartree-Fock tables of Clementi and Roetti [23] for neutral atoms. The distorted wave  $\chi^{(+)}$  for the incoming electrons has been calculated in the exchange potential of the neutral Ca atoms and the outgoing distorted waves  $\chi^{(-)}$  in the potential of Ca ion. Calculations have been carried out with (i) atom potential for the fast (scattered) electron and (ii) with ion potential for fast (scattered) electron. In the calculations

of  $\chi^{(+)}$  and  $\chi^{(-)}$ , the spin average static exchange potential of Furness and McCarthy [20] and the local density potential of Gianturco and Scialla [21] have been used.

The effect of post collision interaction (PCI) has been taken into account by including the parameter  $N_{ee}$ , defined as [18, 22]

$$N_{ee} = \frac{\gamma}{e^\gamma - 1},$$

where,

$$\gamma = \frac{2\pi}{|\mathbf{k}_1 - \mathbf{k}_2|}.$$

The TDCS can now be simply rewritten to incorporate PCI as

$$\frac{d^3\sigma}{d\Omega_1 d\Omega_2 dE_1} = N_{ee} (2\pi)^4 \frac{k_1 k_2}{k_0} \sum_{av} (|f|^2 + |g|^2 - \text{Re}(f^* g)). \quad (4)$$

The exchange potential of Furness and McCarthy [20] is local in character and has been improved upon by Gianturco and Scialla [21] who added a term to account for local momentum of the bound electron, which makes the modified potential less attractive. The exchange potential of Gianturco and Scialla is given by

$$V_E(r) = 0.5 \left[ E - V_D(r) + \frac{3}{10} (3\pi^2 \rho(r))^{2/3} - \left\{ \left[ E - V_D(r) + \frac{3}{10} (3\pi^2 \rho(r))^{2/3} \right]^2 + 4\pi\rho(r) \right\}^{1/2} \right]$$

where  $\rho(r)$  is the electron charge density. The direct distorting potential  $V_D(r)$  is obtained from target radial orbital  $u_{nl}(r)$  (McCarthy [24]) as

$$V_D(r) = \sum_{nl} N_{nl} \int dr' [u_{nl}(r')]^2 / r_{>} \quad (5)$$

where  $r_{>}$  is greater of  $r$  and  $r'$ ,  $N_{nl}$  is the number of electrons in each orbital  $u_{nl}$ . The inclusion of local momentum of the bound electron reduces the local velocity of the incoming electron with the result that the corresponding correlation term weakens the attractive part of the interaction. The modified semiclassical exchange potential (MSCEP) of Gianturco and Scialla [21] has been compared with static exchange potential of Furness and McCarthy [19] for Ca at excess energies of 4 eV and 58.5 eV in Figure 3. It is clear from the figure that the additional term in MSCEP reduces the attractive character of the potential.

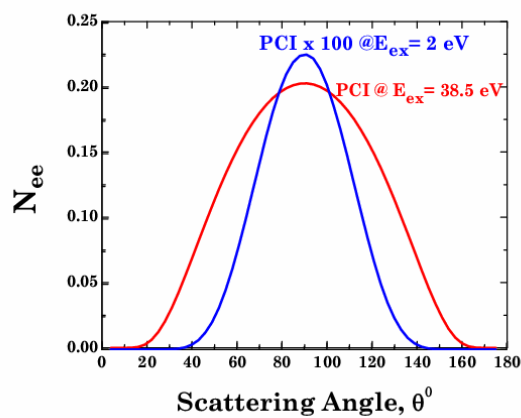


**Figure 2.** Variation of Gamow factor, with scattering angle at two different impact energies for Ca4s.

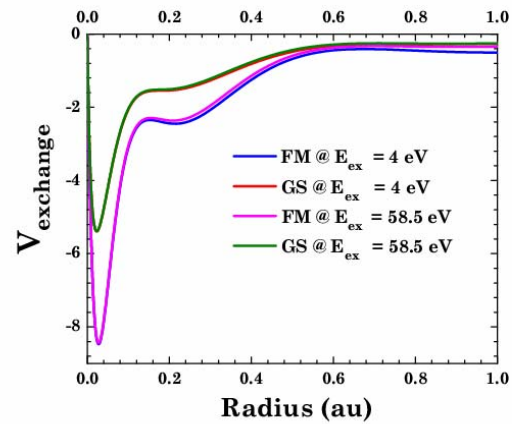


**Figure 3.** Exchange part of potential at the excess energies of (a) 4 eV and (b) 58.5 eV for Ca4s. Blue and Magenta curves represent the static exchange potential [20] and red and green curves represent the modified semiclassical exchange potential [21].

The amplitudes (3) are evaluated in the partial wave form. The number of partial waves required depends upon the incident energy and the orbital. A careful check has been made by calculating the plane wave approximation in which the distorted waves are replaced by plane waves, and then the results are compared with analytical plane wave numbers. While this is a good test of convergence it is not full proof since partial wave convergence of the plane wave approximation can sometimes be more rapid than the distorted wave case. The details about the integration of radial matrix element that is employed in the present work are described in detail by McCarthy [24].

### 3. Results and Discussion

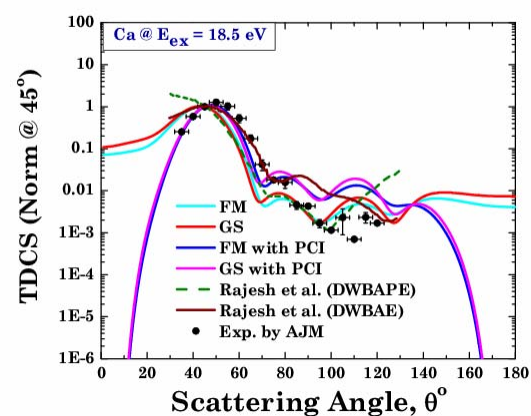
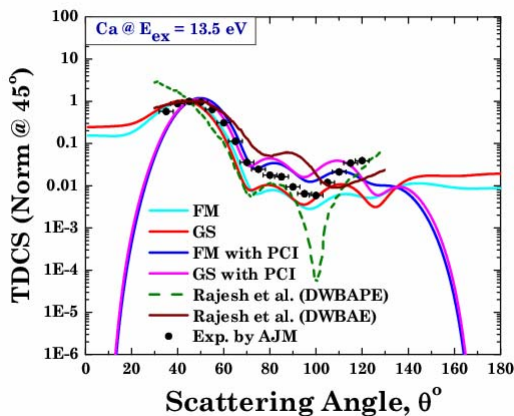
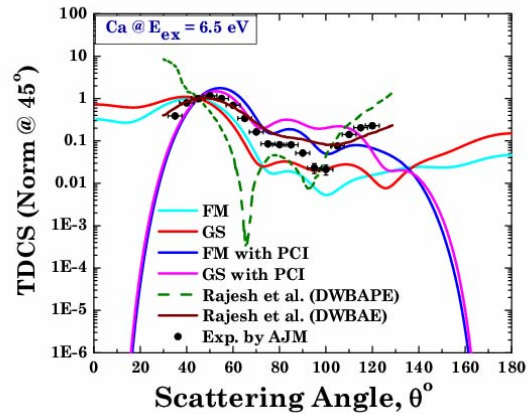
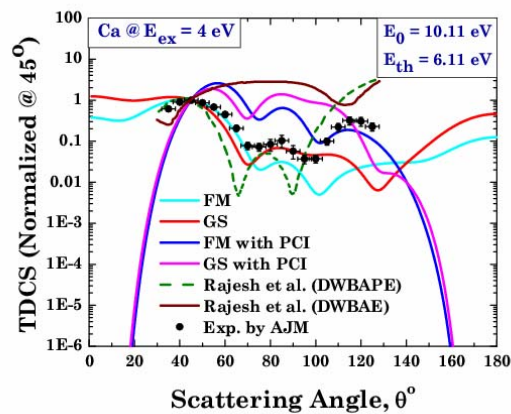
The triple differential cross section (TDCS) for Ca in coplanar symmetric geometry at the excess energies of 4, 6.5, 13.5, 18.5, 28.5, 38.5, 48.5 and 58.5 eV above the ionization threshold are presented in figures 4 (a) - (h), respectively, along with recent experimental data of Murray [12, 13] and the theoretical results of Chauhan et al. [19] for comparison. The results are presented on logarithmic scale because of large variation in the cross section. All the results are in relative magnitudes and are normalized to unity at  $\theta = 45^\circ$ .

The calculations have been carried out with target and ion potentials for the fast electron without taking in to account of the exchange effects, as the exchange amplitude is equal to the direct amplitude for coplanar symmetric kinematics and hence does not have effect on the cross section as can be observed from equation 2. The results with target potential and ion potential are almost the same; hence only the latter is presented here. For the calculations, both the Spin Averaged Static Exchange Potential and Modified Semi Classical Exchange Potential have been used in the present study. The effect of PCI has also been studied via Gamow factor [18, 22] which is a reasonably appropriate way of taking into account the repulsive interaction between the outgoing electrons in coplanar symmetric geometry, as is evident from the form of the factor (Figure 2).

The following features of this geometry are apparent in the present calculations.

- (i) A forward peak at  $\theta \approx 45^\circ$  due to single scattering mechanism
- (ii) A back scattering peak at  $\theta \approx 120^\circ$  due to double scattering mechanism
- (iii) Zero cross section at  $\theta = 0^\circ$  and at  $\theta = 180^\circ$  with PCI, and
- (iv) Increase in ratio of forward to backward scattering peaks with increase in energy

In addition to these, both the present study and experiment display a structure around  $90^\circ$  especially at low energies though the peak is not well pronounced in the experimental results at higher energies.



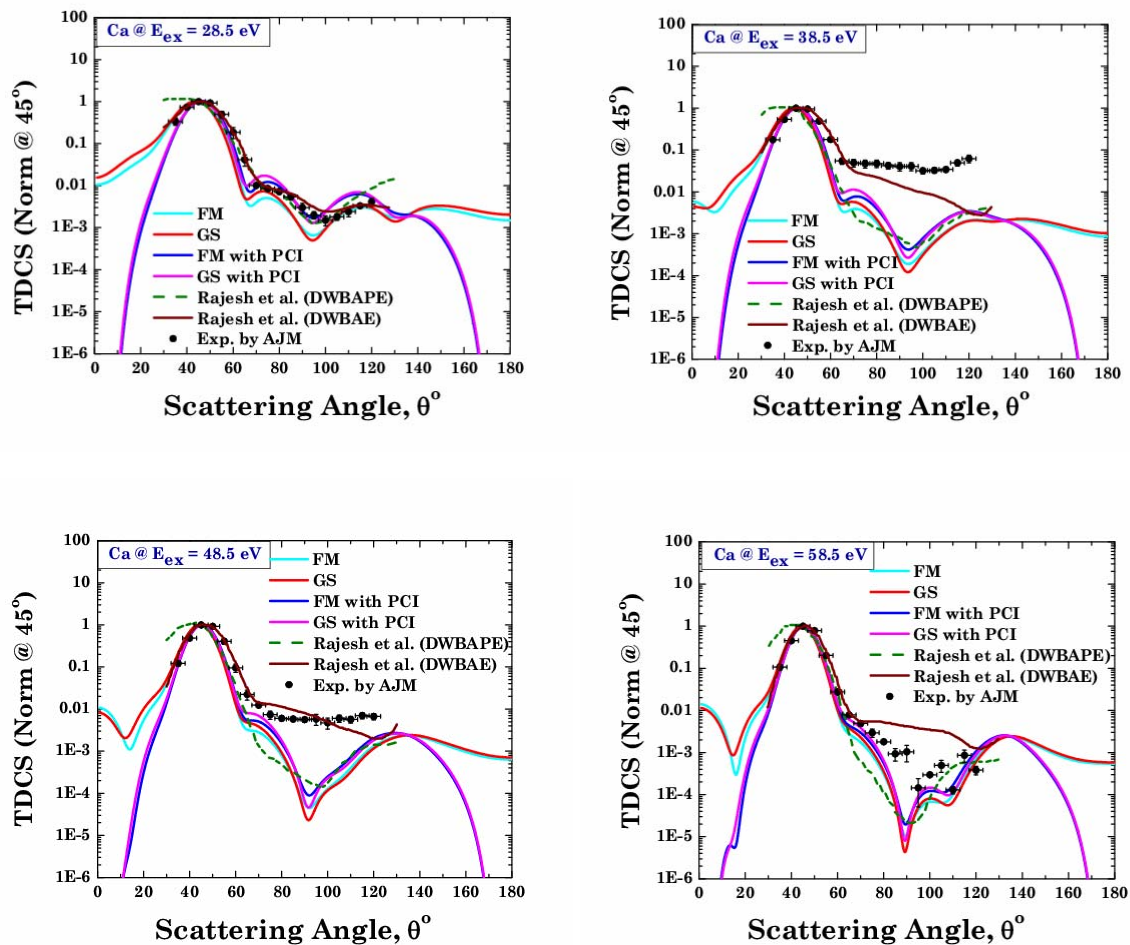


**Figure 4.** Triple differential cross section of  $e^-$ -Ca scattering at excess energies of (a) 4, (b) 6.5 (c) 13.5 (d) 18.5 (e) 28.5 (f) 38.5 (g) 48.5 (h) 58.5 eV. Red and cyan curves represent respectively the present calculations with FM and GS potentials; blue and magenta curves represent those which include PCI; green and brown curves correspond respectively to results due to Chauhan et al. with and without PCI [19], and the dots correspond to experimental results due to Murray et al. [12, 13].

We now compare present theoretical results and the experimental results [12, 13] along with results from the earlier study [19]. The calculations with the spin averaged static exchange potential and those with MSCEP show marked differences only at very low excess energies. It is found that, unlike the results of Chauhan et al. [19], the present results with PCI are almost as good as those without PCI in reproducing the experimental results even in the lower energy region, except for the fact that the calculations with PCI result in vanishing cross section at  $\theta \sim 0^\circ$  and  $\theta \sim 180^\circ$ . The model employed by Chauhan et al. leads to a broad, relatively featureless cross-section at the lowest excess energies 4 eV and 6.5 eV above the threshold, when PCI is absent; whereas a three peak structure emerges once it is included. On the other hand, the present study with both FM and GS potentials reproduces the three peak structure even without PCI, similar to how CCC (Convergent Close Coupling) model [25] predicts. Chauhan et al. used angle dependent effective charges in order to incorporate PCI, but it is apparent that the inclusion of PCI through the Gamow factor is more effective in

reproducing the experimental results. The PCI model using Gamow factor is applicable to the entire angle range while method of angle dependent effective charges is not suitable at scattering angles below  $30^\circ$ . However, it is found that at the lowest energy, namely  $E_{\text{ex}} = 4$  eV, the present model of PCI significantly increases the relative magnitude of the cross section around  $90^\circ$ ; while at higher energies, the present results display almost similar agreement with the experimental results. Also, at higher impact energies, both the previous and the present studies lead to roughly similar behavior, except for the fact that the earlier study is restricted to the angle range  $30^\circ < \theta < 130^\circ$ . The present way of including the PCI using Gamow factor is reasonably expected to work well in the angle range  $\theta \leq 30^\circ$  and  $\theta \geq 140^\circ$ , where the cross section goes to zero very rapidly, as we anticipate from the nature of the post collision interaction between the electrons, which is mainly the long range repulsive coulomb interaction that tends to make the electrons emerge in opposite directions. However, since the experimental results in this region are not yet available, we focus our discussion mainly in the region  $30^\circ < \theta < 130^\circ$ .

We now compare our theoretical study with the experiment in detail. At the excess energy of 4eV, the present results without PCI are in better agreement with the experiment than those include PCI. A similar behavior is observed in our recent study on Mg 3s [26] in the lower energy regime. This is because of the inadequacy of using the simple multiplicative Gamow factor in including PCI. However, at higher excess energies, the DWBAP (DWBA with PCI) is in good agreement with the experimental results except for higher angle regions at certain energies, which we will discuss next.

The major deviation of the theoretical results from the experimental ones occurs at excess energies 38.5eV and 48.5eV, where the experimental cross-section shows nearly structureless behavior at high angle ranges, while all the theoretical results follow the same trend as for other energies. However, at the excess energy of 58.5eV, the experimental results also show a complex behavior, which is more or less in agreement with the theoretical results.

It is interesting to note that, in Mg 3s [26], the cross-section in the regions near threshold shows only forward and backward scattering peaks. The middle peak structure emerges only at excess energies about ten times the threshold value, whereas in Ca 4s, the middle peak is present even very near threshold ( $\sim 1.61$  times). Also, while Mg 3s cross-section has a dip-like structure just below  $30^\circ$ , which is not present at the lowest energy and diminishes as the energy increases, there is no such structure in Ca 4s cross-section except at the highest energy considered. However this needs to be verified by experiment.

#### 4. Conclusions

The DWBA with suitable interaction potential is proved to be reasonably successful in explaining various aspects of the (e, 2e) cross section of Ca in the coplanar symmetric geometry. Both the Spin Averaged Static Exchange Potential and the Modified Semi Classical Exchange Potential reproduce all major features of the cross section in this geometry in better agreement with the experiment compared to previous study [19] over the entire angular range except at certain energies, where the experimental results show unexpected, almost featureless behavior at high angles. The two peaks appearing at  $\theta \approx 45^\circ$  and  $\theta \approx 120^\circ$  in the figures 4 (a)-(h), namely the forward and backward scattering peaks are explained to be arising from single electron-electron binary encounter and double binary collision respectively [27]. The TDCS

with electron-electron repulsion included through Gamow factor shows a vanishing cross section near  $\theta = 0^\circ$  and  $180^\circ$  since it is very unlikely that the outgoing electrons emerge along the same direction. The presence of other minima in TDCS can be explained in terms of the interference among different partial waves which essentially constitute electron wave functions. The present way of including PCI through Gamow factor considerably increases the relative magnitude of the cross section around  $90^\circ$  at the lowest impact energy, i.e., in the very near threshold region, which has been found also from the electron impact ionization study of Mg 3s [26]. Thus, the Gamow factor which serves the purpose of including the effects of post collision interaction between the outgoing electrons can perhaps be modified to obtain better agreement in the near-threshold region. Furthermore, it is not the PCI which is responsible for the three peak structure at the lowest impact energy, in contrast to the result from the earlier study [19].

The present calculations without PCI show better agreement with the experimental results than the theory that includes PCI at the lowest energy, i.e., at  $E_{ex} = 4$  eV. This is evident from the Mg 3s [26] studies also. However, as the energy increases, the results with PCI show analogous agreement. A similar overall comparison with the theoretical and the experimental results for Ca and Mg paves a way for properly modifying the theory, especially in choosing a model to include PCI so that the modified DWBA becomes a more powerful technique in explaining the (e, 2e) process of atomic systems in the whole range of energies and angles. Nevertheless, the Gamow factor could be used to incorporate PCI, but with suitable modification. As the polarization effects are also known to be very important at low energy scattering, the discrepancies found between the present form of modified DWBA and experiment are expected to be diminished by including these effects as well. Further, owing to the unexpected behavior of experimental results at certain energies such as  $E_{ex} = 38.5$ eV and 48.5eV at angle ranges around  $\theta \geq 60^\circ$ , it seems that further experiments at these energies are desirable.

### Acknowledgements

We are thankful to Professor A J Murray for providing his experimental results and for useful discussions.

### References

- [1] Ehrhardt H, Schulz M, Tekaas T, and Willmann K 1969 *Phys. Rev. Lett.* **22** 89
- [2] Jr Amaldi U, Egidi A, Marconero R and Pizzella G 1969 *Rev. Sci. Instrum.* **40** 1001
- [3] Pochat A, Tweed R J, Peresse J, Joachain C J, Piraux B and Byion F W 1983 *J. Phys. B* **16** 775
- [4] Hawley-Jones T J, Read F H, Cvejanovic S, Hammond P and King G C 1992 *J. Phys. B* **25** 2393
- [5] Röder J, Ehrhardt H, Bray I, Farsa D V, and McCarthy I E 1996 *J. Phys. B* **29** 2103
- [6] Murray A J, in (e,2e) and Related process, edited by Whelan C T, Walters H R J, A Lahman-Bennan and Ehrhardt H 1993 P372
- [7] Murray A J and Read F H 1992 *Phys. Rev. Letts.* **69** 2912
- [8] Murray A J and Read F H 1993 *J. Phys. B* **26**, 369
- [9] Murray A J and Read F H 1993 *Phys. Rev. A* **47** 3724
- [10] Murray A J and Read F H 2000 *J. Phys. B* **33** 2859
- [11] Murray A J and Read F H 2000 *J. Phys. B* **33** L297
- [12] Murray A J and Cvejanovic D 2003 *J. Phys. B* **36** 4875
- [13] Murray A J 2005 *Phys. Rev. A* **72** 062711

- [14] Whelan C T, Walters H R J, Allan R J and Zhang X , in ( *e,2e* ) and Related process, edited by Whelan C T, Walters H R J, Lahman-Bennan A and Ehrhardt H 1993 P1
- [15] Khajuria Y and Tripathi D N 1998 *J. Phys. B* **31** 2359
- [16] Allan R J, Whelan C T, and Walters H R J 1993 *Int. symp. on ( e,2e ) collisions, double photoionization and related processes, J. Physique IV* **3** 39
- [17] Rioual S, Pochat A, Gélébart F, Allan R J, Whelan C T, and Walters H R J 1995 *J. Phys. B* **28** 5317
- [18] Whelan C T, Allan R J, Rasch J, Walters H R J, Zhang X, Röder J, Jung K and Ehrhardt H 1994 *Phys. Rev. A* **50** 4394
- [19] Chauhan R K, Srivastava M K and Srivastava R 2005 *Phys. Rev. A* **71** 032708
- [20] Furness J B, and McCarthy I E 1973 *J. Phys. B* **6** 2280
- [21] Gianturco F A, and Scialla S 1987 *J. Phys. B* **20** 3171
- [22] Whelan C T, Allan R J and Walters H R J 1993 in *international symposium on (e,2e) collision, Double photoionization, and related processes, J. Phys. IV* **39**
- [23] Clementi E, and Roetti C 1974 *At. Data Nucl. Data Tables* **14** 177
- [24] McCarthy I E 1995 *Aust. J. Phys.* **48** 1
- [25] Bray I and Stelbovics A T 1992 *Phys. Rev. A.* **46** 6995
- [26] Khajuria Y, Kumar S Sunil and Deshmukh P C 2007 *Phys. Rev. A* **75** 022708
- [27] Walters H R J 1984 *Phys. Rep.* **116** 1